MOLECULAR DYNAMICS SIMULATION OF THE KINETIC REACTION OF Ni AND Al NANOPARTICLES

B. J. Henz[*]
U.S. Army Research Laboratory
Aberdeen Proving Ground, MD 21005

T. Hawa, and M. R. Zachariah
National Institute of Standards and Technology
Gaithersburg, MD 20899
and
Departments of Mechanical Engineering and of Chemistry and Biochemistry
University of Maryland
College Park, MD 20742

ABSTRACT

The U.S. Army has an interest in the use of alloys that produce excessive heat during formation and can be used for structural purposes such as shell casings. Molecular dynamics simulations have been used to provide a more thorough understanding of one of these alloys systems, namely the kinetic reaction of Ni and Al nanoparticles. We have considered the affect of primary particle size on sintering time and sintering temperature for separate nanoparticles and for coated nanoparticles in the form of Ni-coated Al nanoparticles and Al-coated Ni. Simulation results show that the sintering time for coated nanoparticles is linearly dependent upon the number of atoms or volume of the sintering nanoparticles. We have also found that nanoparticle size and surface energy is an important factor in determining the adiabatic reaction temperature.

1. INTRODUCTION

There is considerable interest in the self-propagating high-temperature synthesis (SHS) reactions of intermetallic compounds because of the associated energy release that takes place (Lee, 2005) during the alloying reaction. In addition to the energetic reaction observed in these materials it is possible to produce structural materials that contain this energy release property. Once ignited, the SHS reaction releases a large amount of energy in a short period of time. One significant difference between SHS and typical combustion processes is that the reactants and products are confined to the condensed state (Gennari et al., 2006). The SHS process has many potential applications where heat generation is required and oxygen is not available or gaseous products are not desirable. These include alloy formation, net-shape processing, propellants, and as initiators. One of the compounds formed from the SHS reaction, and studied here, is NiAl or nickel aluminide. NiAl is an important alloy because of its desirable high temperature strength and oxidation resistance (Nash and Kleppa, 2001) and the high energy of formation (Hu and Nash, 2005).

The focus of this paper is to use atomistic simulation to model the reactive behavior of Ni-Al nanoparticles in various configurations. Fortunately, there have been numerous efforts to determine accurate empirical potentials for simulating the Ni-Al material system (Yu et al., 2007). These efforts have primarily focused on bulk materials rather than nanoparticle systems (Delogu, 2007), even though there are many manufacturing processes that produce nanometer sized powders for SHS reactions (Zhu and Abbschian, 2003).

2. SIMULATION APPROACH

In this work we employ classical molecular dynamics (MD) with an EAM interatomic potential to study the SHS reaction. The EAM is used because of its accuracy and capability to scale up to material systems with over 10^6 atoms. The MD simulations are compared with thermodynamic analyses in order to provide validation of the simulation results and assess the expected energy release.

The MD simulation was conducted using the LAMMPS software package (Plimpton, 1995). For the Ni-Al interactions the Finnis-Sinclair EAM potential (Finnis and Sinclair, 1984) from Angelo et al. (Angelo et al., 1995) was used. The Finnis-Sinclair EAM potential allows for non-symmetric embedding potential terms, potentially providing improved accuracy for metallic alloys (Ackland and Vitek, 1990). In addition to the parameters for NiAl from Angelo et al. other authors have also developed parameters for the Ni-Al system (Mishin et al., 2002).

Three primary nanoparticle sizes were considered in this work from smallest to largest are nanoparticles of approximately 3nm, 5nm, and 10nm in size. The

		Form Approved
Report Documentation Page		*OMB No. 0704-0188*

1. REPORT DATE **DEC 2008**	2. REPORT TYPE **N/A**	3. DATES COVERED **-**	
4. TITLE AND SUBTITLE **Molecular Dynamics Simulation Of The Kinetic Reaction Of Ni And Al Nanoparticles**		5a. CONTRACT NUMBER	
		5b. GRANT NUMBER	
		5c. PROGRAM ELEMENT NUMBER	
6. AUTHOR(S)		5d. PROJECT NUMBER	
		5e. TASK NUMBER	
		5f. WORK UNIT NUMBER	
7. PERFORMING ORGANIZATION NAME(S) AND ADDRESS(ES) **U.S. Army Research Laboratory Aberdeen Proving Ground, MD 21005**		8. PERFORMING ORGANIZATION REPORT NUMBER	
9. SPONSORING/MONITORING AGENCY NAME(S) AND ADDRESS(ES)		10. SPONSOR/MONITOR'S ACRONYM(S)	
		11. SPONSOR/MONITOR'S REPORT NUMBER(S)	
12. DISTRIBUTION/AVAILABILITY STATEMENT **Approved for public release, distribution unlimited**			
13. SUPPLEMENTARY NOTES **See also ADM002187. Proceedings of the Army Science Conference (26th) Held in Orlando, Florida on 1-4 December 2008, The original document contains color images.**			
14. ABSTRACT			
15. SUBJECT TERMS			

16. SECURITY CLASSIFICATION OF:			17. LIMITATION OF ABSTRACT **UU**	18. NUMBER OF PAGES **8**	19a. NAME OF RESPONSIBLE PERSON
a. REPORT **unclassified**	b. ABSTRACT **unclassified**	c. THIS PAGE **unclassified**			

Standard Form 298 (Rev. 8-98)
Prescribed by ANSI Std Z39-18

range of sizes was chosen because it represents nanoparticles that may be produced in the laboratory, and which offers reasonable computational time to conduct parametric studies. For the largest system studied, the 10nm diameter nanoparticle kinetic reaction simulation requires approximately two days and 64 processor cores to complete a few nanoseconds of simulated time on 3.0 GHz Intel processors.

3. THERMODYNAMIC ANALYSIS OF SEPARATE NANOPARTICLES

The separate nanoparticle system is used as a model for powder metallurgy systems where Ni and Al particles are compressed into a structural component. In addition to mechanical properties, the structural component will contain stored energy for future release through a SHS reaction. A thermodynamic analysis of the SHS reaction for the separate Ni and Al nanoparticle system is used here to determine the expected trends and data points for simulation validation. In the thermodynamic analysis we are interested in determining the system parameters of the Ni-Al nanoparticle system that contribute to the combustion temperature and reaction time. Here we have assumed an adiabatic process. This is a good approximation since the reaction occurs on relatively short time scales and the nanoparticles are expected to be included in a much larger system where the overall surface to volume ratio is small, limiting convective and radiative heat loss. The SHS reaction of an equimolar Ni and Al mixture is written as

$$0.5Ni + 0.5Al \rightarrow Ni_{0.5}Al_{0.5} \qquad (1)$$
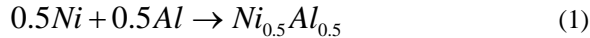
In order to compute the adiabatic temperature for the synthesis reaction the enthalpy of the products and reactants must be equal.

$$H_{prod}(T_{ad}) = H_{reac}(T_0) \qquad (2)$$

We begin the analysis by assuming that the reaction begins with the reactants at 600K, which is above the simulated melting temperature of the Al nanoparticles. The reactant enthalpy includes the enthalpy of solid Ni and liquid Al (Hu and Nash, 2005). The Al nanoparticle is assumed to be liquid, because for small nanoparticles the melting temperature is known to be appreciably below the bulk melting temperature (Pawlow, 1909). Additionally, for the EAM potential used here (Angelo et al., 1995) the aluminum is liquid for these nanoparticle sizes at 600K. The choice of initial temperature will have a nearly linear affect on the adiabatic temperature as long as the initial temperature is between the melting temperature of the Al and Ni nanoparticles. This linear affect has been observed in experiments (Zhu et al., 2003), and is a reasonable assumption so long as the heat capacities of the solid phases of Ni and NiAl are relatively insensitive to temperature in the ranges studied.

For the products of the SHS process the enthalpy calculation must take into account contributions from the melting of the nickel and the NiAl nanoparticle, enthalpy of formation for the NiAl alloy, and changes in surface energy. The first of these, the enthalpies of melting for Ni and NiAl is experimentally determined to be $17.2 \, kJ/_{mol}$ and $31.4 \, kJ/_{mol}$, respectively. The enthalpy of formation that is used here is approximately in the middle of the reported values at about $-65 \, kJ/_{mol}$ (Hu and Nash, 2005; Arroyave).

The last contribution to the enthalpy of the products, results from the change in surface energy, due to the reduced total surface area of the combined nanoparticle (Zachariah et al., 1996), given as equation 3.

$$\Delta E_{surf} = \sigma_{NiAl} \cdot a_{NiAl} - \left(\sigma_{Ni} \cdot a_{Ni} + \sigma_{Al} \cdot a_{Al} \right) \qquad (3)$$

In equation 3, a_{NiAl}, a_{Ni}, and a_{Al} are the surface area of the NiAl, Ni, and Al nanoparticles, respectively. For the 3nm, 5nm, and 10nm Al nanoparticles the reactant surface area is computed from the Gibbs surface (Allen and Tildsesley, 1996) as 36.32 nm^2, 98.17 nm^2, and 343.7 nm^2, respectively. For the associated Ni nanoparticles the surface area is 27.15 nm^2, 73.59 nm^2, and 257.87 nm^2, respectively. The surface energy is approximately $1115 \, mJ/_{m^2}$ for Al and $2573 \, mJ/_{m^2}$ for Ni at 600K (Nizhenko, 2004). The surface area of the sintered NiAl nanoparticles is 50.77 nm^2, 137.18 nm^2, and 480.25 nm^2 for the 3nm, 5nm, and 10nm nanoparticle case, respectively. In experimental analysis of the free surface energy of NiAl near its melting point, the free surface energy has been reported as $1400 \, mJ/_{m^2}$ (Lozovoi et al., 2000).

The approximate change in energy versus nanoparticle size is tabulated in table 1.

Table 1. change in surface energy versus nanoparticle size.

Nanoparticle Radius (nm)	ΔE_{surf} (kJ/mol)
3	-18.35
5	-11.41
10	-6.17

In table 1 the trend is for a lower surface energy contribution to the reaction as the nanoparticle size increases. Intuitively, one may expect this because the surface area to volume ratio is also decreasing with increasing particle size. With the enthalpy of formation for NiAl around $-65\,^{kJ}/_{mol}$, the surface energy contribution to the change in enthalpy for coalescence of 10nm diameter nanoparticles is less than 10% of the total enthalpy change. This means that even at relatively small nanoparticle sizes, e.g. 10nm, the affect of nanoparticle size on energy release is minimal.

With the preceding discussion it is possible to take into account many of the sources of enthalpy change in the reaction products including phase and surface area changes. The enthalpy of the products is now estimated as

$$H_{prod} = H_{form,NiAl} + \Delta H_{surf} +$$

$$\int_{298K}^{T_{ad}} C_{p,NiAl}(T)dT + H_{melt,Ni} \qquad (4)$$

The heat capacity for solid and liquid NiAl is given in Kubaschewski et al., 1993. For the 3nm case, assuming the NiAl nanoparticle melting temperature to be about 1350K, or the melting point of a similarly sized Ni nanoparticle it is possible to compute the adiabatic reaction temperature, table 2.

Table 2. Computed adiabatic temperature versus nanoparticle radius, including contact of flat surfaces or infinitely sized spheres.

Nanoparticle Radius (nm)	T_{ad} (K)
3	2115
5	1920
10	1772
∞	1599

Notice in table 2 that if no surface energy contribution is considered, i.e. infinitely large spheres, the final adiabatic temperature is computed to be 1599K. In the simulation section we will observe that these results are reasonable and accurately predict the simulated increase in temperature attributable to the contribution from the surface energy.

4. THE COALESCENCE PROCESS

For Ni and Al nanoparticles the SHS reaction consists of two processes, namely coalescence and alloying. In this work we have considered the coalescence of a two nanoparticle system with an Al and a Ni nanoparticle atomic ratio of unity. A complete SHS reaction of this system will result in a single NiAl nanoparticle. The MD simulations used in this work models adiabatic conditions with constant number of atoms and total system energy. The purpose of these simulations is to analyze the affect of nanoparticle size on sintering time, adiabatic combustion temperature, and to visualize the process.

The nanoparticle sintering process is driven by two sources of energy as previously discussed. The first of these is a decrease in surface area that lowers the total surface energy of the system. This energy release mechanism is also observed in the sintering of homogeneous material systems such as silicon nanoparticles (Zachariah et al., 1996; Mukherjee et al., 2003). The second source of energy is from the reactive synthesis that occurs initially at the interface between the nanoparticles and later throughout the entire system. The energy release from the surface sintering is proportional to the surface area of the Ni nanoparticle that is coated by Al and in the whole system to the total number of Ni and Al atoms. Additionally, with the temperature increase there is a decrease in the viscosity of the liquid aluminum that will affect the predicted coalescence time.

The coalescence of nanoparticles in the liquid and solid phases has been examined extensively (Lewis et al., 1997; Hawa and Zachariah, 2005, 2006). These studies are primarily concerned with the coalescence of two liquid or two solid nanoparticles. The analysis for the Ni-Al system requires considering the coalescence of a liquid Al nanoparticle and a solid Ni nanoparticle. Lewis et al (Lewis et al., 1997) considered the coalescence of a liquid and a solid gold nanoparticle, this is similar to the situation here except that the material system considered was homogeneous.

In Lewis et al., 1997, the author is able to simulate two phases occurring simultaneously for a single material by choosing the size of each nanoparticle such that at a specific temperature the phase of the nanoparticles is different. Lewis found that coalescence proceeded in two stages, first the contact area was maximized and secondly "sphericization" took place driven by surface diffusion. The first stage is much faster than the second and is very similar to the process observed here where the Al nanoparticle maximizes the contact area and partially coats the Ni nanoparticle. In this case there is an added driving force in addition to the surface energy, specifically the energy release on forming of Ni-Al bonds as compared to the Al-Al and Ni-Ni bonds. During the second stage the atoms in the two nanoparticles diffuse and rearrange until the system becomes a single spherical nanoparticle. This stage is driven strongly by the formation of Ni-Al bonds and is expected to occur on a much shorter time

scale than for two nanoparticles of the same material. The analytical model and MD simulation results shown in the following sections will explore this assumption.

4.1. PHENOMENOLOGICAL MODEL OF NANOPARTICLE REACTIVE SINTERING

To gain further insight we have developed a phenomenological model for the reactive sintering of Ni and Al nanoparticles. The model includes energy release from surface energy, bond formation, and viscous dissipation through deformation. Frenkel (Frenkel, 1945) has developed a model for the coalescence of two homogeneous nanoparticles, however his model did not account for any phase change, kinetic sintering, or heterogeneous materials. We have extended Frenkel's model to consider the coalescence of two liquid drops to consider the coalescence of a liquid and a solid drop with reactive synthesis. The details are elsewhere (Henz, et al., submitted)

The result is that by conservation of energy the rate of coalescence can now be computed by equilibrating the rate of viscous dissipation with the rate of energy release from the surface and the SHS reaction.

$$\frac{dE_{viscous}}{dt} = \frac{dE_{surf}}{dt} + \frac{dE_{reactive}}{dt} \tag{5a}$$

$$\tfrac{8}{3}\pi r_{Al,0}^3 \eta \left(\frac{dD}{dt}\right)^2 =$$

$$\frac{d}{dt}\left[\sigma_{Ni}^s \cdot S_{Ni,\exp osed} + \sigma_{Al}^l \cdot S_{Al,\exp osed}\right]$$

$$+\frac{d}{dt}\left[2\beta\pi v_{Ni} r_{Ni}\right] \tag{5b}$$

After writing equation 5b in terms of dθ/dt and simplifying the right and left hand sides we find that equation 5b is only linearly dependent on dθ/dt. Even with this simplification, equation 5, is most easily solved numerically using an iterative solver. In order to solve equation 5b we need some physical properties of Al, Ni, and NiAl. The dynamic viscosity of bulk molten Al at the melting temperature is about $\eta = 1.3\cdot10^{-3} Pa\cdot s$ (Assal et al., 2006). Based upon a comparison of the configurational energy in MD simulations of separate nanoparticles and Al-coated Ni nanoparticles the energy release per unit area, $\beta_{density}$, is estimated to be $20.7\, {}^{eV}/_{nm^2}$. This number is computed by subtracting the system energy of an Al coated Ni nanoparticle system from the energy of a system with separate nanoparticles and dividing by the interfacial surface area. This method results in the net change in energy during coating of the Ni surface with Al since some Al-Al bonds are lost during the coating process while some Ni-Al bonds are formed at the interface. By numerically solving equation 5b we are able to compute the contact angle, θ, as a function of time and relate this to total exposed surface area of the coalescing nanoparticles. This result is presented in figure 1 along with a comparison to the MD simulation results.
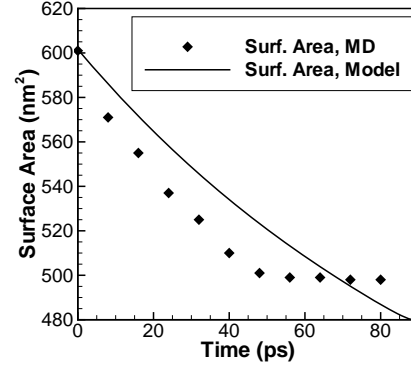

Figure 1. Total system surface area versus time from mathematical model and MD simulations for the sintering of 10nm diameter nanoparticles, where the final surface area of the NiAl nanoparticle is approximately 480 nm^2.

Although qualitatively the results in figure 1 show similar trends the absolute rate of coalescence is slightly under predicted by the model. This difference can be attributed to the obvious simplicity of the model and more specifically to the difficulty in obtaining accurate material parameters. For instance, it is difficult to compare the viscosity of a nanoparticle to the bulk material (Zachariah and Carrier, 1999) and since the coalescence time is linearly dependent upon the viscosity a change in viscosity is directly proportional to a change in modeled coalescence time. Additionally, the energy release per unit area term assumes that the net change in energy due to the addition of Ni-Al bonds at the interface is a constant value. This is likely not completely accurate since fewer Al bonds must be broken to form new Ni-Al bonds during the initial contact of the nanoparticles. However, the deviation in this energy release term is likely to be minimal. The deviation of the model time from the simulation results at about 50 ps is due to the switch from stage 1 to stage 2 in the kinetic coalescence process as described by Lewis et al (Lewis et al., 1997). As described by Lewis, during stage 2, surface diffusion is the predominant factor in continued coalescence and is a much slower process than contact area maximization. The actual simulation

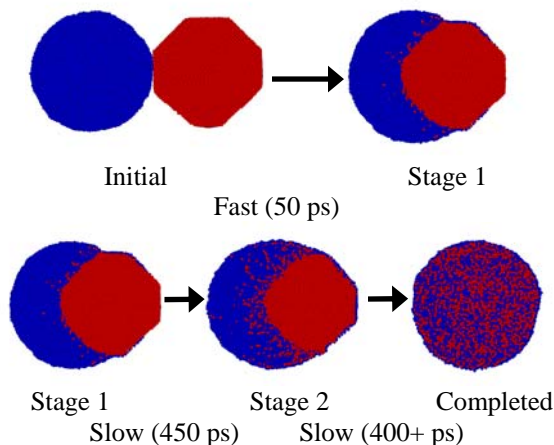results of the observed coalescence process are given in figure 2.

Figure 2. Cross sectional view from MD simulations of Ni/Al nanoparticle sintering process showing the start of the second stage of coalescence where diffusion is the driving force as opposed to contact area maximization. Aluminum atoms are blue and nickel atoms are red.

In figure 2 each of the steps in the coalescence process are illustrated by MD simulation results of the coalescence of 10nm diameter Al and Ni nanoparticles. The correlation of the sintering stages to the reaction temperature and time is illustrated in figure 3. In the initial step the liquid Al nanoparticle, blue atoms in figure 2, has melted and is spherical in shape. The solid Ni nanoparticle, red atoms, has large faceted sides, a typical configuration for a crystalline nanoparticle at low temperatures. During stage 1 the Al nanoparticle is attracted to the Ni surface because of the dual driving forces of surface energy minimization and Ni-Al bond formation. This period lasts about 50 ps. Between stages 1 and 2 the driving forces associated with the surface energy are counteracted by a resistance to flow in the Al nanoparticle, causing the coalescence process to slow down dramatically. During stage 2, lasting about 450 ps, the surface area is not changing so that energy release from the surface energy terms has ceased to be a contributing energy term. The subsequent energy release is entirely attributable to the formation of Ni-Al bonds. This stage lasts a much longer time than the initial nanoparticle coalescence stage and is governed by the material diffusion coefficients. Initially at stage 2 the Ni nanoparticle is still solid and the formation of Ni-Al bonds is only possible by Al diffusing into the Ni core or Ni on the surface of the core melting and diffusing away from the interface. This process proceeds until the Ni core has reached its melting point at which time coalescence proceeds more

rapidly, driven by the enthalpy of formation of NiAl. From stage 2 until complete alloying has occurred, taking approximately 400 ps, diffusion and mixing of Ni and Al atoms is the primary driving force.
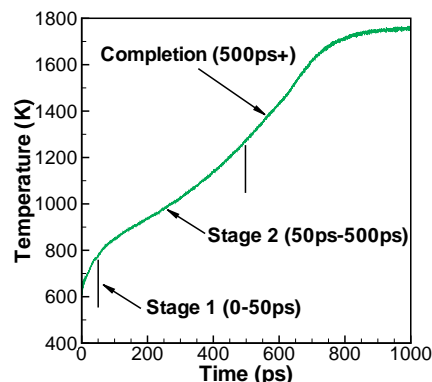

Figure 3. Time versus temperature plot for sintering of separate 10nm diameter Al and Ni nanoparticles. The various stages if the coalescence processes are denoted on the curve, including the final completion stage that occurs after the Ni nanoparticle has melted.

4.2. MD SIMULATION RESULTS OF SEPARATE NANOPARTICLE REACTIVITY

In figure 4, the MD simulation results for thesintering of separate equimolar nanoparticles are plotted along with the computed adiabatic temperature for each considered particle size.
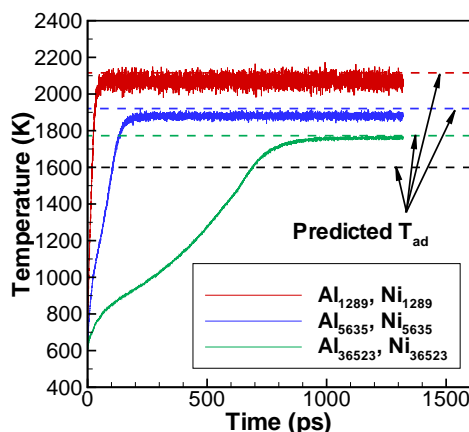

Figure 4. Temperature versus time in the sintering of nanoparticles with an Ni:Al ratio of 1:1. The subscripts in the legend refer to the number of atoms of each material and correspond to nanoparticles of diameter approximately 3nm, 5nm, and 10nm. The color coded dashed lines are the computed adiabatic temperature from the thermodynamic analysis. The black dashed line is the predicted temperature for coalescence of bulk Al and Ni.

From figure 4 it is apparent that the predicted adiabatic temperature is in close agreement with the simulated temperature. Variability of the computed temperature arises from the wide range of experimental results for the surface tension for liquid Al and solid Ni, the reported enthalpy of formation for NiAl, and the assumed melting temperature for the Ni and NiAl materials at this scale. Each of these experimental data points are used in the thermodynamic analysis and contribute to the small inaccuracies in the predicted temperature.

The characteristic time for reactive synthesis that we use here is defined by Zhao et al (Zhao et al., 2006) as t when

$$T(t) = T_0 + 0.8(T_1 - T_0) \qquad (6)$$

where T_0 is the initial temperature, T_1 is the maximum size dependent temperature reached, and $T(t)$ is the transient temperature. The computed reaction times demonstrate that the time required for separate nanoparticles to react has a power law relationship that is between nanoparticle volume (3), and surface area (2). This implies that not only will the reaction temperature be higher, but will occur more rapidly with decreases in particle size, to a power of about 2.5. This is important because a high rate of energy release is desirable for many applications.

5. REACTIVE SINTERING OF CORE-SHELL NANOPARTICLES

5.1. ALUMINUM COATED NICKEL

In this section we will discuss the sintering process for an Al-coated Ni nanoparticle followed by a discussion of a Ni-coated Al nanoparticle. Both of these systems can be used as a model for highly compacted Ni and Al nanoparticles or one material serving as a matrix for nanoaprticles of the other. In the first model system we assume that a Ni nanoparticle has been coated with Al and equilibrated without the Ni melting, or any further reaction occurring. Results for the reaction time and temperature will be presented and a comparison with the separate nanoparticle case will be given. Here again we have considered three system sizes with 1289, 5635, and 36523 atoms each of Al and Ni.

An initial estimate is that the coalescence process for the fully coated nanoparticle system will be a truncated version of the separate nanoparticle case. In the coated nanoparticle system we do not have the first stage of coalescence occurring and only observe

the second stage, namely diffusion of Ni and Al atoms to form Ni-Al bonds. The sintering temperature versus time plot is given in figure 5 and shows an interesting result. Whereas the maximum temperature reached increases with decreasing nanoparticle size for coalescence of separate nanoparticles, the opposite is true here, the temperature decreases with decreasing nanoparticle size.
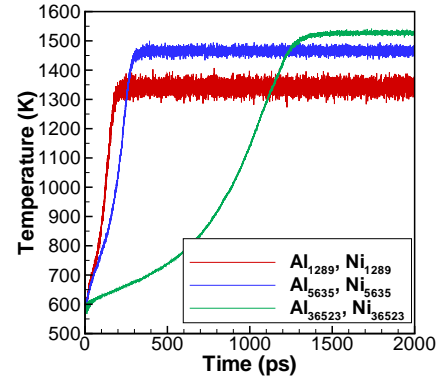

Figure 5. Temperature versus time in the sintering of Al-coated Ni nanoparticles with an Ni:Al ratio of 1:1.

In figure 5 the observed decrease in adiabatic temperature is due to the fact that the ratio of atoms near the interfacial region to the atoms in the bulk nanoparticle decreases as the nanoparticle size increases. Atoms in the interfacial region have already formed Ni-Al bonds and are therefore already at a lower configurational energy than if they were contained in a homogeneous nanoparticle of either pure Al or Ni. If we extend the adiabatic temperature relationship to infinitely large particles we would approach the result obtained from the analysis of separate nanoparticle as they increase in size. The thermodynamic analysis is similar except that the surface energy term is zero and the enthalpy of formation is lowered by a factor proportional to the ratio of surface area to volume. The enthalpy of the products for coated nanoparticles becomes

$$H_{prod} = \left(1 - \frac{t \cdot A_{surface}}{V}\right) H_{form,NiAl} +$$

$$\int_{298K}^{T_{ad}} C_{p,NiAl}(T)\,dT + H_{melt,Ni} \qquad (7)$$

where t is a computed thickness value for the interfacial layer, $A_{surface}$ is the area of the interfacial region, and V is the volume of the Ni core. In order to determine the correct empirical thickness value, t, for equation 7 we have used the adiabatic temperature

computed in the MD simulation results for the Al-coated Ni nanoparticle. These results indicate that an interface thickness of 0.07nm is able to accurately predict the adiabatic temperature observed in the MD simulations, figure 6.
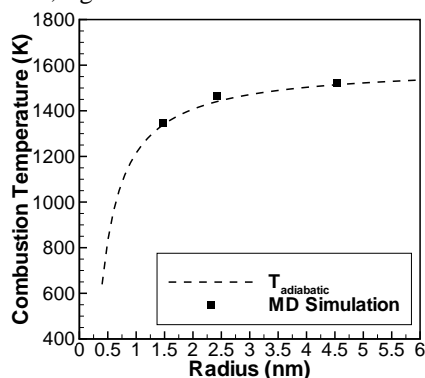

Figure 6. Comparison of thermodynamically determined adiabatic temperature for Al-coated Ni nanoparticle and results from MD simulation.

In figure 6 it is apparent that the adiabatic combustion temperature is highly size dependent for nanoparticles of less than 10nm in diameter. For very small nanoparticles, less than 1nm diameter, there is little predicted change in temperature from the initial temperature of 600K since most of the potential Ni-Al bonds have already been formed.

From the sintering of separate nanoparticles it is expected that the reaction time will be related to the radius of the nanoparticle to a power of about 2.5. In figure 7 this appears to be the case for this range of nanoparticle sizes. A slight deviation from the separate nanoparticle result is most likely related to the fact that the coalescence process, stage 1, is not included in this model system and diffusion takes longer to initialize the kinetic reaction process.
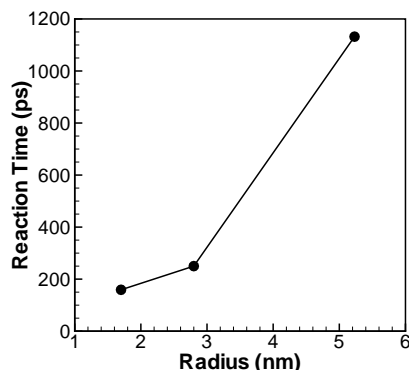

Figure 7. Reaction time versus number of Al atoms in the Al-coated Ni nanoparticle system.

The results for the Al-coated Ni nanoparticle indicate the trends that one might expect from a material system that included an Al matrix with embedded Ni nanoparticles. From the results in figures 6 and 7 there are two competing reaction results, namely reaction time and maximum temperature. In figure 7 we see that as the Ni nanoparticle size decreases the reaction time decreases, causing the energy release rate to increase. A second observation that can be made from figure 6 is that the reaction temperature decreases with decreasing Ni nanoparticle size, potentially minimizing the effect of the rapid energy release.

Looking more closely at the reaction time versus number of atoms for the separate nanoparticle and Al-coated Ni nanoparticle cases we observe a similar relationship of reaction time to nanoparticle size as that found in separate nanoparticles. In both cases the reaction time appears to have a power law relationship with radius, with an exponent of 2.5.

CONCLUSIONS

We have analyzed two model systems for the energetic reaction of Ni and Al. In the first case we considered the coalescing and sintering of separate nanoparticles and found that the energy release from the change in surface area is only significant at small, less that 10 nm diameter, nanoparticles. These separated nanoparticle reaction simulations and thermodynamic analyses show that the reaction time will decrease and the adiabatic reaction temperature will increase with decreasing nanoparticle sizes. This may be important for applications where high energy release rates are desired.

In the second part of this work we considered the sintering of Al-coated Ni nanoparticles as a model material system for nanoparticles embedded in a matrix of the other metal. This work revealed that the reaction time is again inversely related to nanoparticle size but the adiabatic temperature decreases with decreasing nanoparticle size. Mechanically the Al-coated Ni nanoparticle system is a model system for a light weight Al matrix with embedded Ni nanoparticles, a system with relatively high strength compared to a loosely bonded powder of Al and Ni nanoparticles. This Al matrix system could be used in systems where mechanical strength is important in addition to energy release from kinetic sintering of the Ni and Al atoms.

REFERENCES

Ackland, G. J., and Vitek, V. "Many-body potentials and atomic-scale relaxations in noble-metal alloys", *Physical Review B*, **41**(15), 10324–10333, 1990.

Allen, M. P. and Tildesley, D. J. <u>Computer Simulation of Liquids</u>. New York: Oxford, 1996.

Angelo, J. E., Moody, N. R., and Baskes, M. I. "Trapping of hydrogen to lattice defects in nickel", *Modelling Simul. Mater. Sci. Eng.*, **3**, 289–307, (1995).

Arroyave, R., Shin, D., and Liu, Z.-K. "Ab initio thermodynamic properties of stoichiometric phases in the Ni–Al system", *Acta Materialia*, **53**, 1809–1819, 2005.

Assael, M. A., Kakosimos, K., Banish, R. M., Brillo, J., Egry, I., Brooks, R., Quested, P. N., Mills, K. C., Nagashima, A., Sato, Y., and Wakeham, W. A. "Reference Data for the Density and Viscosity of Liquid Aluminum and Liquid Iron", *J. Phys. Chem. Ref. Data*, **35**(1), 285–300, (2006).

Chrifi-Alaoui, F. Z., Nassik, M., Mahdouk, K., and Gachon, J. C. "Enthalpies of formation of the Ni–Al intermetallic compounds", *Journal of Alloys and Compounds*, **364**, 121–126, 2004.

Delogu, F. "Numerical simulation of the thermal response of Al core/Ni shell nanometer-sized particles", *Nanotechnology*, **18**, 505702, 2007.

Finnis, M. W. and Sinclair, J. E. "A simple empirical N-body potential for transition metals", *Philosophical Magazine A*, **50**, 45–55 (1984).

Frenkel, J. *J. Phys.*, **9**, 385, (1945).

Gennari, S., Tamburini, U. A., Maglia, F., Spinolo, G., and Munir, Z. A. "A new approach to the modeling of SHS reactions: Combustion synthesis of transition metal aluminides", *Acta Materialia*, **54**, 2343–2351, (2006).

Hawa, T. and Zachariah, M. R. "Coalescence kinetics of bare and hydrogen-coated silicon nanoparticles: A molecular dynamics study", *Physical Review B*, **71**, 165434, 2005.

Hawa, T. and Zachariah, M. R. "Coalescence kinetics of unequal sized nanoparticles", *Aerosol Science*, **37**, 1–15, 2006.

Henz, B. J., Hawa, T., and Zachariah, M. R. "Molecular Dynamics Simulation of the Kinetic Reaction of Ni and Al Nanoparticles", *Journal of Applied Physics*, (submitted).

Hu, R. and Nash, P. "The enthalpy of formation of NiAl", *Journal of Materials Science*, **40**, 1067–1069, 2005.

Kubaschewski, O., <u>Materials Thermochemistry, 6th ed.</u>, Pergamon Press, New York, (1993) 299.

Lewis, L. J., Jensen, P., and Barrat, J.-L. "Melting, freezing, and coalescence of gold nanoparticles", *Physical Review B*, **56**(4), 2248–2257, 1997.

Li, H. P. "Influence of ignition parameters on micropyretic synthesis of NiAl compound", *Materials Science & Engineering A*, **404**, 146–152, 2005.

Lozovoi, A. Y., Alavi, A., and Finnis, M. W. "Surface Stoichiometry and the Initial Oxidation of NiAl(110)", *Physical Review Letters*, **85**(3), 610–613, 2000.

Mishin, Y., Mehl, M. J., and Papaconstantopoulos, M. A. "Embedded-atom potential for B2-NiAl", *Physical Review B*, **65**, 224114, (2002).

Mukherjee, D., Sonwane, C. G., and Zachariah, M. R. "Kinetic Monte-Carlo Simulation of the Effect of Coalescence Energy Release on the Size and Shape Evolution of NanoParticles Grown as an Aerosol", *Journal of Chemical Physics*, **119**, 3391, 2003.

Nash, P., and Kleppa, O. "Composition dependence of the enthalpies of formation of NiAl", *Journal of Alloys and Compounds*, **321**, 228–231, 2001.

Nizhenko, V. I. "Free Surface Energy as a Criterion for the Sequence of Intermetallic Layer Formation in Reaction Couples", *Powder Metallurgy and Metal Ceramics*, **43**(5–6), 273–279 (2004).

Pawlow, P. *Z Phys. Chem.*, **65**, 545, 1909.

Plimpton, S. J. "Fast Parallel Algorithms for Short-Range Molecular Dynamics", *Journal of Computational Physics*, **117**, 1–19, 1995.

Yu, S., Wang, C.-Y., Yu, T., and Cai, J. "Self-diffusion in the intermetallic compounds NiAl and Ni_3Al: An embedded atom method study", *Physica B*, **396**, 138–144, 2007.

Zachariah, M. R., and Carrier, M. J. "Molecular Dynamics Computation of Gas-Phase Nanoparticle Sintering: A Comparison with Phenomenological Models", *Journal of Aerosol Science*, **30**(9), 1139–1151, 1999.

Zachariah, M. R., Carrier, M. J., and Blasiten-Barojas, E., *J. Phys. Chem.* **100**, 14856 (1996).

Zhao, S., Germann, T. C., and Strachan, A. "Atomistic simulations of shock-induced alloying reactions in Ni/Al nanolaminates", *Journal of Chemical Physics*, **125**, 164707, (2006).

Zhu, P., Li, J. C. M., and Liu, C. T. "Adiabatic temperature of combustion synthesis of Al-Ni systems", *Materials Science and Engineering A*, **357**, 248–257, 2003.

Zhu, H. X. and Abbaschian, R. "Reactive processing of nickel-aluminide intermetallic compounds", *Journal of Materials Science*, **38**, 3861–3870, 2003.